

## THE ABUNDANCE OF VERY LARGE HYDROCARBONS AND CARBON CLUSTERS IN THE DIFFUSE INTERSTELLAR MEDIUM

R. P. A. BETTENS

Department of Physics, Ohio State University, Columbus, OH 43210-1106

AND

ERIC HERBST

Departments of Physics and Astronomy, Ohio State University, Columbus, OH 43210-1106

Received 1995 October 24; accepted 1996 April 2

### ABSTRACT

Two current gas-phase chemical models of interstellar clouds have been extended to include hydrocarbons and bare carbon clusters through 64 carbon atoms in size. The new molecules comprise linear, monocyclic, tricyclic, and fullerene/ane species but do not include polycyclic aromatic hydrocarbons (PAHs). The reaction networks used to produce and destroy these species have been adopted from a laboratory synthesis of fullerenes. The models have been used to investigate the chemistry of complex molecules in a number of dispersive clouds, which begin as dense clouds but end up as diffuse material. The calculated abundances of large molecules are discussed in terms of candidates for the carriers of the diffuse interstellar bands (DIBs). We find that both gas-phase models utilized can produce large abundances of 64 carbon atom species, considered to represent molecules of this size and larger. Such species are DIB candidates only if the abundances are not spread too thinly over many species. One of the two gas-phase models used leads to large abundances of fullerenes and fulleranes. If this model is accurate, the fullerenes/anes represent reasonable candidates for the carriers of the DIBs. If small hydrocarbon “seeds” are assumed to be present on dust particles and to photodesorb during cloud dispersion, we find that large abundances of linear and monocyclic hydrocarbons can also be produced and maintained via gas-phase chemistry, so that these molecules become additional DIB-carrier candidates.

*Subject headings:* ISM: abundances — ISM: clouds — ISM: molecules — molecular processes

### 1. INTRODUCTION

Current gas-phase chemical models of dense interstellar clouds contain molecules through  $\approx 10$  atoms in size (Herbst & Leung 1989, 1990; Bettens, Lee, & Herbst 1995). Presently, there are two chemical models, called by us the new standard model (hereafter NSM) and model 4 (hereafter M4), that account for most of the abundances of the polyatomic species seen in dark clouds such as TMC-1 to within an order of magnitude at an early time of  $10^5$  yr (Bettens et al. 1995). In the NSM, ion-molecule reactions are largely responsible for complex molecule formation, while in M4, rapid neutral-neutral reactions play a very significant role. Most of the latter reactions have not been studied in the laboratory; their rates are based on experiments on a few selected systems (Sims & Smith 1995). It is not possible with our present understanding of neutral-neutral reactions at low temperatures to rule out either model. In general, the predicted drop-off in abundance with increasing molecular complexity is less with the M4 reaction set. A third chemical model, the new neutral-neutral model, includes neutral-neutral reactions to an even greater extent than M4, but does not reproduce the observed polyatomic chemistry in dark clouds (Bettens et al. 1995). Model M4 differs from the new neutral-neutral model in that reactions between atomic oxygen and bare carbon clusters  $C_n$  are assumed not to proceed for  $n > 2$ . This assumption has been verified for the  $n = 3$  case by Woon & Herbst (1996).

We have recently extended the NSM and M4 reaction networks to include the formation and depletion of a large number of bare carbon clusters and unsaturated hydrocarbons through 64 carbon atoms in size (Bettens & Herbst

1995). It might seem foolhardy at this point to extend our networks when there is so much uncertainty in their construction. It is an important problem, however, to determine the feasibility of producing very large molecules in the gas phase under assorted interstellar conditions, with reasonable assumptions about the rate coefficients involved. Moreover, the synthesis of the very large molecules is firmly grounded in the laboratory work of von Helden, Gotts, & Bowers (1993) and Hunter et al. (1994) on fullerene production, although most of the needed rate coefficients and product branching fractions were estimated with the help of the Rice-Ramsperger-Kassel-Marcus (RRKM) statistical technique (Bettens & Herbst 1995; Herbst 1996). Details of the reaction network extension are to be found in our previous paper (Bettens & Herbst 1995). Despite the large number of reactions, the formation and destruction reactions for each individual hydrocarbon are few in number and represent some well-studied laboratory processes (see Table 3 of Bettens & Herbst 1995). The synthesis of complex hydrocarbons proceeds first through the growth of linear species via C and  $C^+$  insertion and association reactions. Once they reach 24 carbon atoms in size, the linear species spontaneously convert into monocyclic rings. The monocyclic rings then grow in size and associate with each other to form tricyclic rings, which continue to grow. Fullerenes are formed via conversion reactions between small ions and tricyclic rings.

The extended models have been used to calculate abundances of complex molecular species under static physical conditions and under conditions in which the dense clouds disperse to form diffuse material. In this paper we focus attention on the latter (dispersive) conditions to test the

possibility that complex hydrocarbons grown in the interstellar medium could be the carriers of the visible diffuse interstellar bands (DIBs), seen in absorption toward reddened stars (Herbig 1993). In order for locally grown large hydrocarbon species to exist in the diffuse interstellar medium, their precursors must first be synthesized in an environment shielded from the interstellar radiation field (ISRF), because, while the larger molecules are stable to the ISRF according to statistical considerations, the smaller species are not. The precursors can be regarded as “seeds.” A variety of classes of complex hydrocarbons and carbon clusters have been suggested as the cause of the DIBs, including linear chains (Douglas 1977), polycyclic aromatic hydrocarbons (PAHs) (Van der Zwet & Allamandola 1985; Léger & d’Hendecourt 1985; Crawford, Tielens, & Allamandola 1985), fullerenes (Webster 1992a, 1992b, 1992c, 1993), and highly unsaturated linear hydrocarbon radicals (Fulara et al. 1993). Most recently, Foing & Ehrenfreund (1994) have reported the controversial identification of  $f\text{-C}_{60}^+$  as the carrier of two of the DIBs (Maier 1994). The neutral buckminsterfullerene molecule,  $f\text{-C}_{60}$ , is not responsible for the diffuse bands; moreover, observations show it to not be a dominant species in diffuse interstellar space (Snow & Seab 1989; Somerville & Bellis 1989).

To date, there have only been two simplified models published for the synthesis of large hydrocarbon species in the interstellar medium (Herbst 1991; Thaddeus 1994). Herbst’s model, designed for dense clouds, contains fixed abundances of hydrocarbon species with fewer than 10 carbon atoms equal to their peak early time abundances in the standard calculation given in Herbst & Leung (1989) and Herbst & Leung (1990), and does not distinguish among the structures and hydrogen content of larger hydrocarbons. Generic reaction rates were assumed for a variety of reaction classes. The results show that only for favorable values of important rate coefficients can sizeable abundances be produced for hydrocarbon molecules 20–30 carbon atoms in size.

In Thaddeus’ model, the synthesis of large bare carbon species occurs efficiently via  $\text{C}^+$ –carbon cluster association reactions and electron-ion sticking reactions in diffuse clouds, even though photodestruction is a significant loss mechanism. The model contains the seed  $\text{C}_{12}$ , a species given an abundance ratio of  $[\text{C}_{12}]/[\text{C}^+] = 10^{-4}$ . A steady state solution is achieved after  $\sim 10^5$  yr, with a maximum in the  $\text{C}_n$  distribution occurring at  $n \sim 20$  and a rapid decline in this distribution at  $n \sim 30$ .

Neither of these models contains a detailed description of the ion-molecule and neutral-neutral chemistry leading to very complex hydrocarbons and clusters. Although the models discussed here are of the detailed variety, most of the rate coefficients utilized remain to be corroborated in the laboratory. This does not mean that they are guessed. The fullerene synthesis is based on laboratory studies. The intermediate species are formed and destroyed by small numbers of reactions, which are analogous to classes of ion-molecule and neutral-neutral reactions involving smaller reactants. Great care has been exercised in determining relevant heats of formation by an assortment of quantum chemical techniques, and product branching ratios have been calculated by the best available statistical techniques. The network, quantum chemical, and rate calculations have appeared in the chemical literature (Bettens & Herbst 1995). Of course, uncertainties exist, mainly in the

nature of the neutral-neutral chemistry, since without potential surfaces for each reaction, activation energy barriers or their absence cannot be determined. That is why two very different basic models have been utilized (Bettens et al. 1995)—one in which neutral-neutral reactions play a small role (NSM) and one in which they play a large role (M4). Extension of these models leads to very different answers regarding the abundances of the fullerenes/fullerenes, showing the uncertainty in our approach more effectively than by simply varying individual rate coefficients, possibly unphysically, to determine the sensitivity of our results to the rate coefficients in a particular network. Previous studies of sensitivity to changes in rate coefficients have yielded mixed results (Herbst & Leung 1986; Roueff 1996).

The remainder of the paper is organized as follows. In § 2 we briefly discuss some aspects of our chemical networks as well as the dynamical conditions assumed. In § 3 the results of our models containing only gas-phase reactions are discussed, with an emphasis on very large species and fullerenes. In § 4 we consider the changes that occur to our chemical models if seed molecules are continually released from grain surfaces. Finally, in § 5 we summarize our results.

## 2. MODELS AND DYNAMICS

As discussed by Bettens & Herbst (1995), the new species in our chemical networks consist of the following molecules: linear neutral and ionic hydrocarbons ( $l\text{-C}_n\text{H}_m$ ,  $n = 10\text{--}23$ ,  $m = 0\text{--}2$  and  $l\text{-C}_n\text{H}_m^+$ ,  $n = 10\text{--}23$ ,  $m = 0\text{--}3$ ); monocyclic rings ( $m\text{-C}_n\text{H}_m$ ,  $n = 24\text{--}64$ ,  $m = 0\text{--}2$  and  $m\text{-C}_n\text{H}_m^+$ ,  $n = 24\text{--}64$ ,  $m = 0\text{--}3$ ); tricyclic rings ( $t\text{-C}_n\text{H}_m$ ,  $n = 48\text{--}64$ ,  $m = 0\text{--}2$  and  $t\text{-C}_n\text{H}_m^+$ ,  $n = 48\text{--}64$ ,  $m = 0\text{--}3$ ); and fullerenes ( $f\text{-C}_n$ ,  $n = 46\text{--}60$ ,  $62\text{--}64$  and  $f\text{-C}_n\text{H}_m^+$ ,  $n = 46\text{--}60$ ,  $62\text{--}64$ ,  $m = 0\text{--}3$ ). Partially hydrogenated neutral fullerenes (fullerenes) have not been included in the models because of space limitations. That some hydrogenation can occur is evident from the results of Petrie et al. (1992) that up to three hydrogen atoms attach themselves to  $f\text{-C}_{60}^+$  with large rate coefficients. In our models this hydrogenation in ions is lost via dissociative recombination reactions, which are assumed to form bare fullerene neutrals plus hydrogen atoms. In addition to the above classes of molecules, we have added the negative ions  $l\text{-C}_n\text{H}_m^-$ ,  $n = 10\text{--}23$ ,  $m = 0, 1$ , since these species possess large electron affinities and may play a synthetic role. The specific formation and destruction reactions for the negative ions are listed in Table 1.

The extension in Bettens & Herbst (1995) was intended to be appended to model M4 and contains a variety of rapid neutral-neutral reactions, although, as in M4, reactions between atomic oxygen and bare carbon clusters  $\text{C}_n$  are assumed not to proceed for  $n > 2$ . For an analogous extension to the NSM network (Bettens et al. 1995),  $\text{O-C}_n$  reactions were included with a rate coefficient of  $5 \times 10^{-11} (T/300)^{1/2} \text{ cm}^3 \text{ s}^{-1}$  and the other neutral-neutral reactions involving complex species eliminated. The resulting reaction sets both contain 1030 chemical species, and include 9780 and 9905 reactions for the NSM and M4 networks, respectively. These networks are available from the authors.

The 64 carbon atom species, the largest molecules in the model, represent the “edge” of our chemical model and are an artificial sink for carbon because no chemical or photo-

TABLE 1

RATE COEFFICIENTS  $k = A \exp(-BA_V)$  FOR NEGATIVE ION-MOLECULE REACTIONS

Reactants	Products	$A^a$	$B^a$
$\text{I-C}_n + e$	$\text{I-C}_n^- + h\nu$	$1.00 \times 10^{-7}$	0.000
$\text{I-C}_n\text{H} + e$	$\text{I-C}_n\text{H}^- + h\nu$	$2.00 \times 10^{-7}$	0.000
$\text{I-C}_n^- + h\nu$	$\text{I-C}_n + e$	$4.97 \times 10^{-9}$	1.748
$\text{I-C}_n\text{H}^- + h\nu$	$\text{I-C}_n\text{H} + e$	$3.39 \times 10^{-9}$	2.001
$\text{I-C}_n^- + \text{C}$	$\text{I-C}_{n+1} + e^b$	$1.00 \times 10^{-9}$	0.000
$\text{I-C}_n + \text{H}$	$\text{I-C}_n\text{H} + e$	$1.00 \times 10^{-9}$	0.000
$\text{I-C}_n\text{H}^- + \text{C}$	$\text{I-C}_{n+1}\text{H} + e^b$	$1.00 \times 10^{-9}$	0.000
$\text{I-C}_n\text{H}^- + \text{H}$	$\text{I-C}_n\text{H}_2 + e$	$1.00 \times 10^{-9}$	0.000

<sup>a</sup>  $A$  has units of  $\text{cm}^3 \text{s}^{-1}$  except for photodetachment where it has units of  $\text{s}^{-1}$ .  $B$  is in units of  $\text{mag}^{-1}$ .

<sup>b</sup> For  $n = 23$  the product is monocyclic.

chemical process destroys them. They effectively contain material that goes on to form larger, more complex hydrocarbons. The fullerene  $\text{f-C}_{60}$  and fullerane ions  $\text{f-C}_{60}\text{H}_m^+$ ,  $m = 0-3$  are also sinks for carbon because molecules in this group cannot leave it. The association between  $\text{C}^+$  and  $\text{f-C}_{60}$  has been measured to occur in the laboratory (Christian, Wan, & Anderson 1992) but is not included in the models because we assume that the product ion is sufficiently loosely bound that it reacts to form  $\text{f-C}_{60}$  and  $\text{C}$  upon recombination with electrons, unlike other large ions, which tend to stick to electrons (Bettens & Herbst 1995). Since hydrogenation is not followed for neutral fullerenes, calculated abundances of  $\text{f-C}_{60}$  and other neutral fullerenes represent the sum of abundances for both these species and fullerane species of the type  $\text{f-C}_n\text{H}_m$ .

In all models the assumed initial physical conditions are  $T = 10 \text{ K}$ ,  $n_i = 2n(\text{H}_2)_i = 2 \times 10^4 \text{ cm}^{-3}$ , and  $(A_V)_i = 20 \text{ mag}$ . The assumed initial relative abundances are given in Table 2.

We consider dynamical models in which a spherical dark cloud of initial radius  $l_i$ , which has undergone  $t_d$  yr of static chemical evolution, expands at constant temperature with a constant radial velocity of  $v_d$ . Rather than continue indefinitely to unphysically low densities, the expansion occurs so as to reach asymptotic final values of gas density  $n_f$  and visual extinction  $(A_V)_f$ . For convenience, we have chosen the physical parameters  $t_d = 0 \text{ yr}$ ,  $n_f = 0.1 \text{ cm}^{-3}$ ,  $(A_V)_f = 0 \text{ mag}$ , and  $v_d = 1 \text{ km s}^{-1}$  as the standard parameters. The initial cloud radius can be obtained by using the standard relationship between the total column density and visual

TABLE 2

INITIAL RELATIVE ABUNDANCES<sup>a</sup>

Element	Relative Abundance
$\text{H}_2$	$5.00 \times 10^{-1}$
$\text{He}$	$1.40 \times 10^{-1}$
$\text{C}^+$	$7.30 \times 10^{-5}$
$\text{N}$	$2.14 \times 10^{-5}$
$\text{O}$	$1.76 \times 10^{-4}$
$e$	$7.31 \times 10^{-5}$
$\text{S}^+$	$8.00 \times 10^{-8}$
$\text{Si}^+$	$8.00 \times 10^{-8}$
$\text{Fe}^+$	$3.00 \times 10^{-9}$
$\text{Na}^+$	$2.00 \times 10^{-9}$
$\text{Mg}^+$	$7.00 \times 10^{-9}$
$\text{P}^+$	$3.00 \times 10^{-9}$
$\text{Cl}^+$	$4.00 \times 10^{-9}$

<sup>a</sup> Relative to the number density of  $\text{H}$ .

extinction to cloud center. The equations for gas density and visual extinction after  $t$  yr of expansion are

$$l = l_i + v_d t, \quad (1)$$

$$n = (n_i - n_f) \left( \frac{l_i}{l} \right)^3 + n_f, \quad (2)$$

$$A_V = [(A_V)_i - (A_V)_f] \left( \frac{l_i}{l} \right)^2 + (A_V)_f. \quad (3)$$

Figure 1 illustrates the diminution of  $n$  and  $A_V$  with time for a cloud with the standard physical parameters. Although these parameters will be emphasized, we have run the NSM and M4 reaction sets with a variety of dynamical parameters, which are tabulated in Table 3, as well as for static diffuse and dark clouds. The “dispersive” models 1–5 studied differ in radial velocities (the standard cloud is referred to as dispersive model 2); the higher the number assigned to the model, the larger the radial expansion velocity. Dispersive cloud model 6 possesses the same expansion velocity as model 5 but starts its expansion after  $t_d = 10^5 \text{ yr}$  of chemical evolution, while models 1–5 all have  $t_d = 0 \text{ yr}$ . The dispersive models eventually lead to very low-density gas. We have also run an “expanded” cloud model with  $t_d = 10^5 \text{ yr}$  and an asymptotic visual extinction of unity and gas density of  $10^2 \text{ cm}^{-3}$  (the so-called “expanded cloud”) representing a moderate density diffuse cloud. The models with large radial velocities are obviously somewhat artificial in the sense that low-temperature conditions would not be expected to prevail. Nor do such conditions even apply to

TABLE 3

PHYSICAL PARAMETERS FOR DYNAMICAL MODELS<sup>a</sup>

$n_i^b$ ( $\text{cm}^{-3}$ )	$n_f$ ( $\text{cm}^{-3}$ )	$(A_V)_i$ (mag)	$(A_V)_f$ (mag)	$t_d^c$ (yr)	$v_d^d$ ( $\text{km s}^{-1}$ )	Comment
$10^4$	$10^{-1}$	20	0	0	0.1	Dispersive cloud 1
$10^4$	$10^{-1}$	20	0	0	1	Dispersive cloud 2
$10^4$	$10^{-1}$	20	0	0	10	Dispersive cloud 3
$10^4$	$10^{-1}$	20	0	0	100	Dispersive cloud 4
$10^4$	$10^{-1}$	20	0	0	1000	Dispersive cloud 5
$10^4$	$10^{-1}$	20	0	$10^5$	1000	Dispersive cloud 6
$10^4$	$10^2$	20	1	$10^5$	10	Expanded cloud

<sup>a</sup> All models were run with  $T = 10 \text{ K}$ .

<sup>b</sup> The subscripts  $i$  and  $f$  represent the initial and final physical conditions, respectively.

<sup>c</sup> The time at which expansion of a dark cloud commences.

<sup>d</sup> The expansion radial velocity.



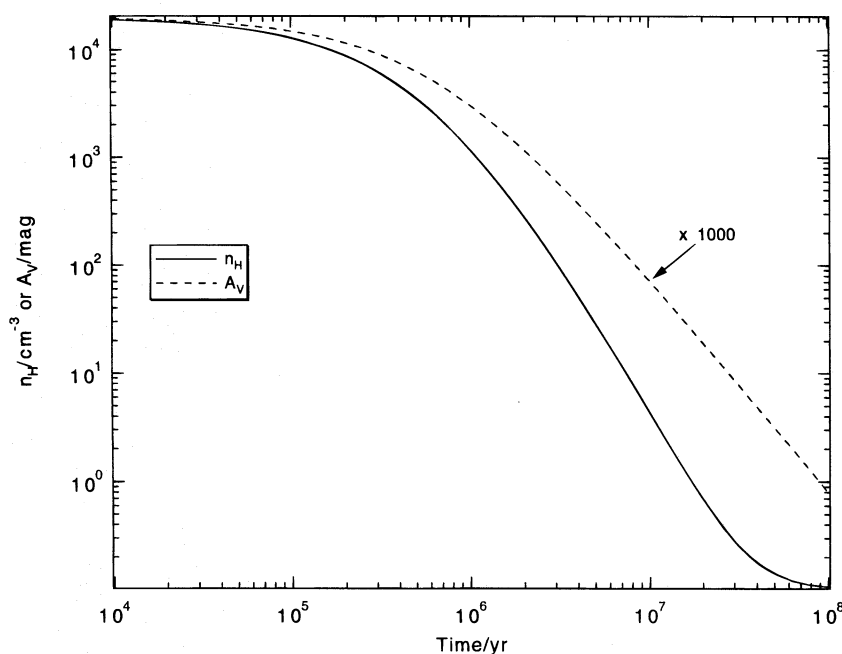


FIG. 1.—Plot of the number density and visual extinction vs. time for the standard physical parameters

the asymptotic values of the dispersive models, although the effect of varying the temperature is minimal.

Our models do not take into account the self-shielding of CO. This process is important in clouds with intermediate visual extinction, where our rate coefficient describing the photodissociation of this species is very different from a more accurate value. In the dynamical models considered here, however, CO self-shielding will have a negligible effect on the abundances of the complex species, because in going from a dark cloud to diffuse conditions, the cloud passes through the regime where self-shielding is important in a relatively short period of time.

### 3. RESULTS: PURELY GAS-PHASE MODELS

In dispersive models with  $t_d = 0$  yr, the gas-phase chemistry can be divided into three eras. In the first, or synthetic, era the chemistry proceeds in a manner similar to that of a dark cloud as long as the diminution of visual extinction and gas density proceed slowly enough. For example, with the standard dynamical parameters, the gas density remains above  $10^3 \text{ cm}^{-3}$  for 1 Myr, which is a long enough time for the gas-phase chemistry to synthesize a wide variety of species. The next era, the expansion era, occurs when there is an increase in the abundance of atomic carbon as  $A_V$  drops rapidly from its initial value and the CO produced in the synthetic era is photodissociated. Finally, when most of the CO has been destroyed and the amount of neutral atomic carbon becomes less than the amount of  $\text{C}^+$ , the dispersion era is reached. On a logarithmic timescale, the point at which the physical conditions change most rapidly is just after the synthetic era, and this time can be regarded as the timescale for expansion.

The distinctive chemical eras are shown in Figure 2, where we plot the fractional abundances of  $\text{C}^+$ , C, CO, and a representative complex species  $\text{m-C}_{30}\text{H}$  versus time for the standard model parameters and the extended NSM reaction set. During the synthetic era, the initial  $\text{C}^+$  is con-

verted into C on the timescale of several hundred years and then more slowly into CO on a timescale of several hundred thousand years. In this era, complex molecule growth occurs as seen by the abundance of  $\text{m-C}_{30}\text{H}$ , although the fractional abundance  $f$  of this rather large molecule is not very great. During the expansion era, the burst of neutral and then ionized atomic carbon heralds another growth period for the complex molecules, and the abundance of  $\text{m-C}_{30}\text{H}$  increases. It is in the first two eras that very large species must be synthesized, because the precursor species are unstable in the ISRF, to which they will be increasingly exposed in the dispersion era. The relationship between photodissociation rate and size has been considered in detail in our previous paper (Bettens & Herbst 1995). In general, at a size exceeding 30–40 carbon atoms, our calcu-

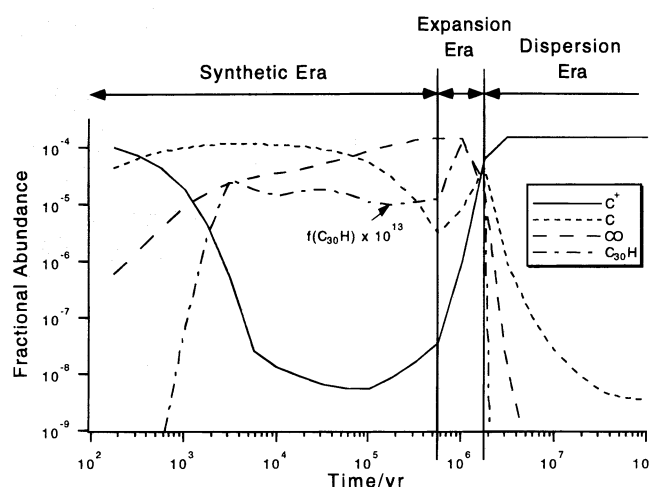


FIG. 2.—Plot illustrating the various chemical eras in dispersive clouds. Shown are the fractional abundances of  $\text{C}^+$ , C, CO, and  $\text{m-C}_{30}\text{H}$  (with respect to  $n/2$ ) vs. time for the standard physical parameters using the extended NSM reaction set.

lations show that hydrocarbon species become entirely resistant to the ISRF, except for photoionization, which is unaffected by size. During the dispersion era, any material not already in a photostable species is returned to  $C^+$ . At the same time, the species large enough to be stable against photodissociation continue to grow in complexity, albeit slowly because of the low densities, until finally all of these stable species are converted into either the large reservoir species  $f-C_{60}$  and  $f-C_{60}H_m^+$  or the 64 carbon atom reservoir species.

The fractional abundances for the linear ( $n \leq 23$ ) and monocyclic  $C_nH$  species are plotted versus time in Figure 3 using the standard physical parameters but with the more powerfully synthetic M4 model. It is clear from Figure 3 that efficient buildup of complex hydrocarbons occurs during the synthetic and expansion eras to fractional abundances of  $10^{-10}$  or greater, but within a short period into the dispersion era virtually all of these hydrocarbons are destroyed. Since the  $m-C_nH$  species are assumed to not react with atomic oxygen, they achieve larger temporary abundances than do the linear radicals, despite their greater size.

The standard parameters are not unique; we have found that under all conditions studied and with both reaction sets that once the dispersion era is reached, rapid destruction of the nonreservoir hydrocarbons occurs. The situation is the same for the “expanded cloud,” where rapid destruction of the hydrocarbons occurs soon after diffuse cloud conditions are reached. In addition, we cannot make any large abundances of complex molecules under static diffuse cloud conditions because we cannot grow precursor “seed” molecules. Therefore, with our present understanding of

purely gas-phase chemistry, linear or monocyclic hydrocarbons with fewer than 64 carbon atoms cannot be sustained at observable levels in the diffuse interstellar medium.

### 3.1. Very Large Hydrocarbons ( $n = 64$ ) and Fullerenes

Figure 4 shows the sum of the fractional abundances for all of the 64 carbon atom species versus time using the NSM (Fig. 4a) and M4 (Fig. 4b) extended reaction sets under assorted physical parameters, including dispersive clouds 1–6 and a static dense cloud. Details of the dense cloud chemistry will appear in a separate publication. Figure 4a clearly illustrates the extra boost in the abundances of the large complex species that occurs during the expansion era for most of the dispersive clouds compared with the static dense cloud. This enhancement occurs to such an extent that we find approximately 0.1% of all carbon (by mass) in these species for clouds 1–3. For clouds 4 and 5, insufficient abundances of seed molecules are produced during the (short) synthetic era. Because cloud 6 evolves chemically as a dark cloud for  $10^5$  yr before expansion commences, its fractional abundance curve coincides with that of the dark cloud for this time.

In Figure 4b, which illustrates results using the extended M4 model, there is little enhancement shown for the dispersive models in the abundances of large complex hydrocarbon species relative to a dense cloud. Moreover, the synthesis is highly efficient compared with the NSM reaction set; approximately 4% of all carbon ends up in these very large hydrocarbon species for dispersive clouds 1–3 and for a dark cloud.

For both networks, we conclude that observable amounts of very large hydrocarbon species can be produced

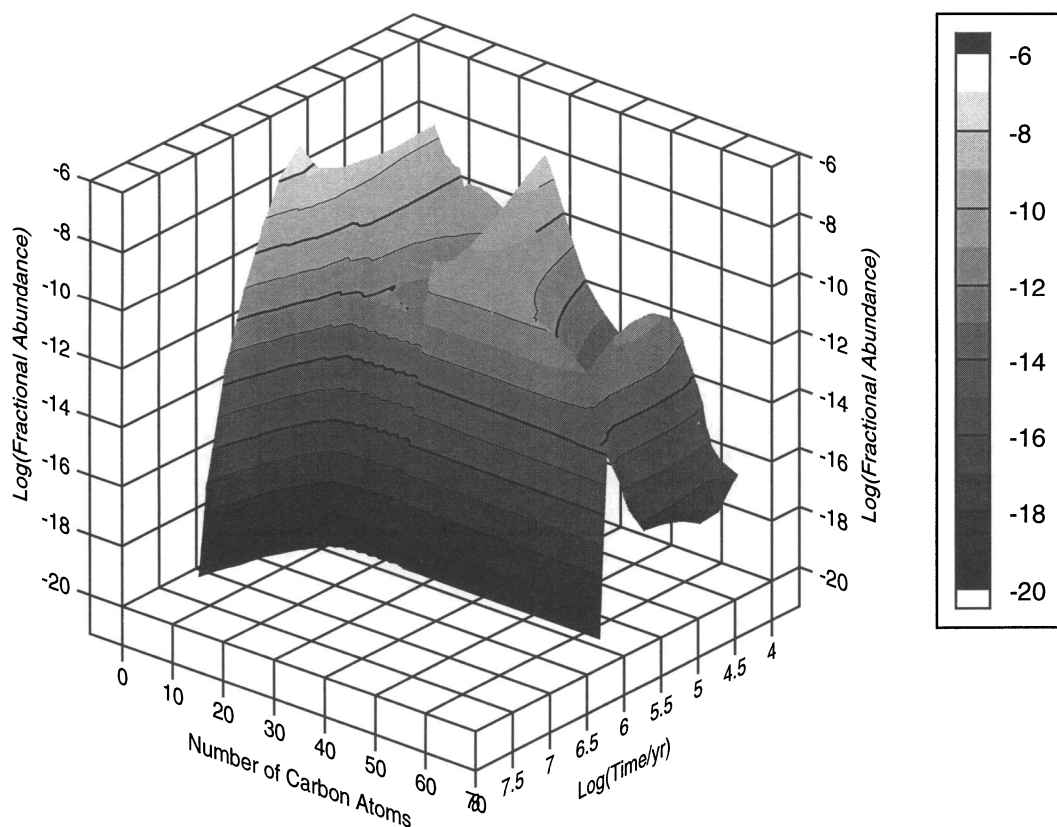


FIG. 3.—Plot of the logarithm of the fractional abundance of  $C_nH$  with respect to  $n/2$  vs. the logarithm of time and vs. number of carbon atoms ( $n$ ) for the linear and monocyclic species using the extended reaction set M4 and standard physical parameters (dispersive cloud 2).

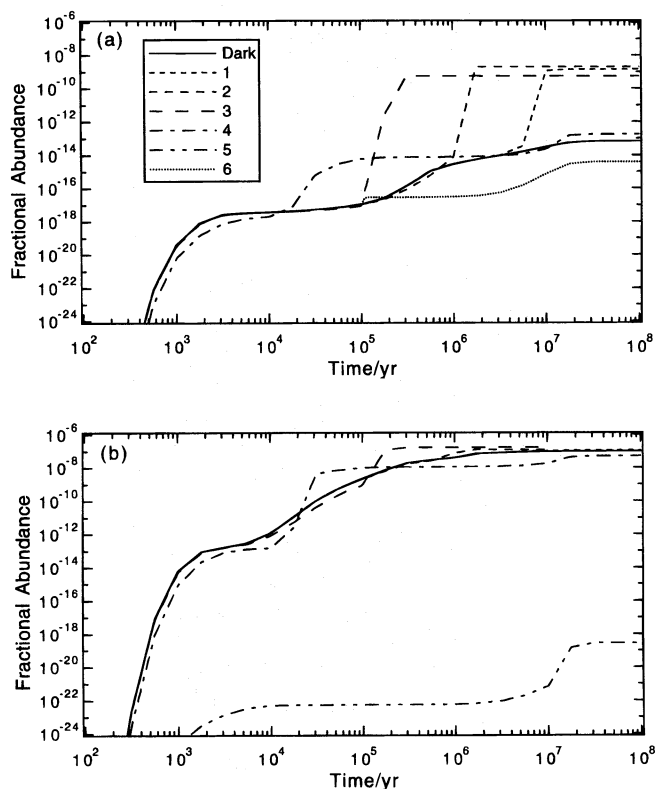


FIG. 4.—Sum of the fractional abundances of 64 carbon atom species vs. time for dispersive clouds 1–6 and a static dark cloud with the extended (a, upper trace) NSM and (b, lower trace) M4 reaction sets.

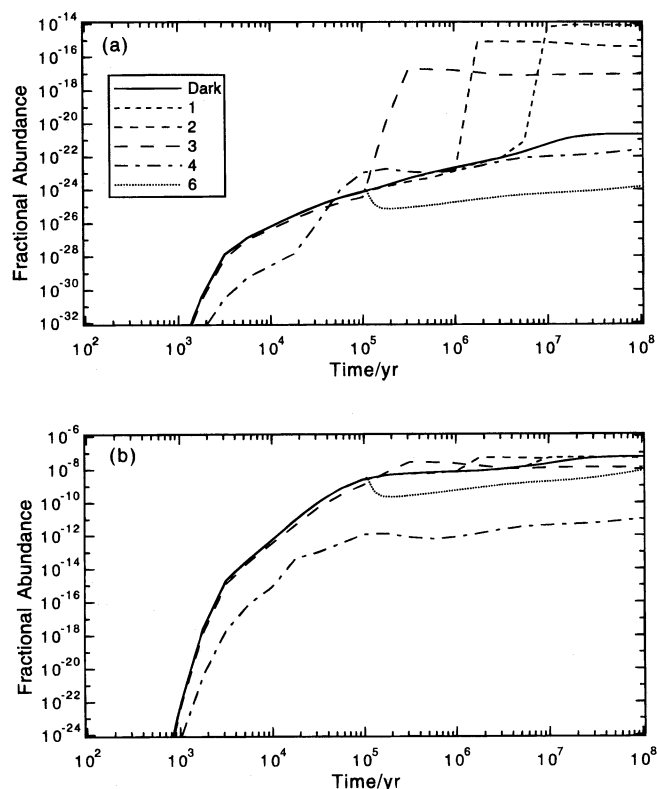


FIG. 5.—Fractional abundance of  $f\text{-C}_{60}$  vs. time for dispersive clouds 1–4, 6, and a static dark cloud with the extended (a, upper trace) NSM and (b, lower trace) M4 reaction sets.

except for very large cloud expansion velocities, provided that the calculated abundances are not smeared out over a very large number of species. Upon examination of the individual abundances of the 64 carbon atom species, we find that the vast majority of this material is in the monocyclic form. However, it is not clear that the dominant very large hydrocarbon species will, in reality, be in this isomeric form because of (1) our neglect of pathways to the formation of PAH molecules, and (2), our model truncation. It may be that much of the complex material ends up in the form of small amorphous carbonaceous grains.

Figure 5 shows the fractional abundance of the sink species  $f\text{-C}_{60}$  (representing  $f\text{-C}_{60}\text{H}_m$  molecules) versus time for different physical parameters using the extended NSM (Fig. 5a) and M4 (Fig. 5b) reaction sets. This figure bears a strong resemblance to Figure 4; with the NSM reaction set, the calculated abundance of this dominant fullerene species is enhanced dramatically during the expansion era for all but the most rapidly dispersive cloud models and then remains at the higher level during the dispersion era since  $f\text{-C}_{60}$  is a sink species. With the M4 reaction set, enhancement during the expansion era does not occur; the time dependence of the abundance is the same as that calculated for a static dark cloud for most of the dispersive cloud models.

It is of significance that the NSM reaction set does not produce more than  $10^{-14}$  fractional abundance of  $f\text{-C}_{60}$ , while calculated abundances for other fullerenes ( $f\text{-C}_n$ ,  $n \neq 60$ ) are far less during the dispersion era. On the other hand, a fractional abundance of  $5 \times 10^{-8}$  is produced for  $f\text{-C}_{60}$  with the M4 reaction set in dispersive clouds 1–3. This accounts for about 2% of the total carbon in our model. We

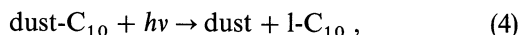
conclude that if reaction set M4 is a reasonably accurate description of the chemistry leading to the formation of fullerenes/fulleranes, then it is quite possible that  $f\text{-C}_{60}\text{H}_m$  species could be carriers of the DIBs.

With an oscillator strength of 0.1, the reported results of Foing & Ehrenfreund (1994) lead to a fractional abundance for  $f\text{-C}_{60}^+$  of  $\approx 2 \times 10^{-9}$ . A value this large can be reproduced at late times (dispersion era) for our standard dispersive cloud as well as for dispersive clouds 1, 3, and 6, as long as the extended M4 reaction network is used. The ion is produced via photoionization of the bare neutral so that our calculated large abundance for the ion is contingent upon our assumption that dissociative recombination leads mainly to the bare  $f\text{-C}_{60}$  precursor and not to fulleranes. With this assumption, the model predicts a very large fractional abundance of pure  $f\text{-C}_{60}$  (see above). Negative observations of Snow & Seab (1989) have shown, however, that a maximum column density of  $10^{14} \text{ cm}^{-2}$  for  $f\text{-C}_{60}$  exists in front of several reddened stars, which we estimate leads to fractional abundances for this species  $\leq$  a few times  $10^{-8}$ , a value somewhat smaller than our model predictions if all the calculated  $f\text{-C}_{60}$  is indeed the bare fullerene. It is possible, moreover, that the dominant fullerene neutrals and ions with 60 carbon atoms are at least partially hydrogenated. If the electron recombinations with the species  $f\text{-C}_{60}\text{H}_m^+$ ,  $m = 1\text{--}3$  are assumed to be associative, then neither  $f\text{-C}_{60}\text{H}_m$  nor  $f\text{-C}_{60}\text{H}_m^+$ ,  $m = 0\text{--}2$  should be observed. In this case, all the material in the 60 carbon atom fullerenes/fulleranes will reside in the fulleranes  $f\text{-C}_{60}\text{H}_3$  and  $f\text{-C}_{60}\text{H}_3^+$ , which might be observable if hydrogenation proceeds no further.



## 4. RESULTS: SEED MOLECULES ON GRAINS

In the dispersive and expanded cloud models, we are not able to synthesize and maintain high abundances of linear and monocyclic hydrocarbons under diffuse conditions. Such molecules may be abundant under such conditions if smaller seed molecules are continually present, as suggested by Thaddeus (1994). To obtain a continuous source of a seed molecule, we have assumed that  $\text{l-C}_{10}$  is initially present on grain surfaces and can be photodesorbed:



with a rate coefficient  $k(\text{s}^{-1})$  given by the expression

$$k = Ae^{-BA\nu}, \quad (5)$$

where the  $B$  parameter is fixed at  $1 \text{ mag}^{-1}$ , reflecting the fact that desorption can occur over a wide variety of wavelengths. The  $\text{l-C}_{10}$  molecule represents a variety of smaller organic species. Its desorption has been incorporated into the extended NSM reaction set, which has been run under both diffuse cloud and expanded cloud conditions. The latter cloud starts from early time chemical abundances achieved in a dark cloud and expands into a diffuse cloud with a density of  $10^2 \text{ cm}^{-3}$ . The seeding of diffuse clouds with  $\text{C}_4\text{H}_2$  molecules has been discussed by Hall & Williams (1995).

The  $A$  parameter in equation 5 was varied from  $1 \times 10^{-9} \text{ s}^{-1}$  to  $1 \times 10^{-15} \text{ s}^{-1}$  in steps of factors of 100, representing a range from efficient to inefficient photodesorption. We chose two initial abundances for  $\text{dust-C}_{10}$ :  $10^6 f(\text{dust})$  and  $10^7 f(\text{dust})$ , where  $f(\text{dust})$  is the fractional abundance of the dust with respect to  $n/2$ ,  $2.64 \times 10^{-12}$ . It should be noted that this is a significant amount of material to be desorbed, the former being 5.6%, and the latter being 56% of the total initial amount of carbon in the gas phase. In terms of monolayers, the former corresponds to one monolayer of material.

In order for the seed to be effective, it must not be depleted too soon. With an  $A$  parameter of  $10^{-15} \text{ s}^{-1}$ , the half-life for depletion of adsorbed  $\text{C}_{10}$  is 22 Myr, and the fractional abundance of this species on grain surfaces does not drop to 1% until  $1.5 \times 10^8 \text{ yr}$ . We find that high abundances of linear and monocyclic hydrocarbons can be sustained for 100 Myr with this small value for  $A$ . In Figure 6 we show the fractional abundances of the linear and monocyclic  $\text{C}_n\text{H}$  species versus  $n$  at  $10^7 \text{ yr}$  under expanded cloud conditions. The results are shown in the absence of seeds, and using  $f(\text{dust-C}_{10}) = 10^6$  and  $10^7 f(\text{dust})$ . Here we can clearly see the enhancement in the abundances of these species with respect to the model without seeds. It can also be seen that increasing  $f(\text{dust-C}_{10})$  by an order of magnitude produces a similar increase in the hydrocarbon abundance. Using the physical conditions of the diffuse cloud, we find the results to be almost identical at  $10^7 \text{ yr}$  to the expanded cloud. Although the linear and monocyclic  $\text{C}_n\text{H}$  radicals are not abundant on an absolute basis, the situation is different for the  $\text{C}_n\text{H}_2$  species, where, in these models, all linear species larger in size than  $\text{C}_9\text{H}_2$  have a fractional abundance of  $\geq 10^{-12}$  with the smaller value of  $f(\text{dust-C}_{10})$ . More hydrogenated species are not followed in our models. Given our results, unsaturated linear and monocyclic molecules cannot be ruled out as likely candidates to be the carriers of the DIBs if the assumption of such a large initial abundance of adsorbed seed molecules makes any sense.

## 5. SUMMARY

We have run a variety of gas-phase chemical models with extended reaction sets in an attempt to determine what complex molecules are the most likely candidates to be the carriers of the DIBs. The networks of reactions used produce linear hydrocarbons and bare clusters through 23 carbon atoms in size. With  $\geq 24$  carbon atoms, these species then spontaneously convert into monocyclic rings. Associ-

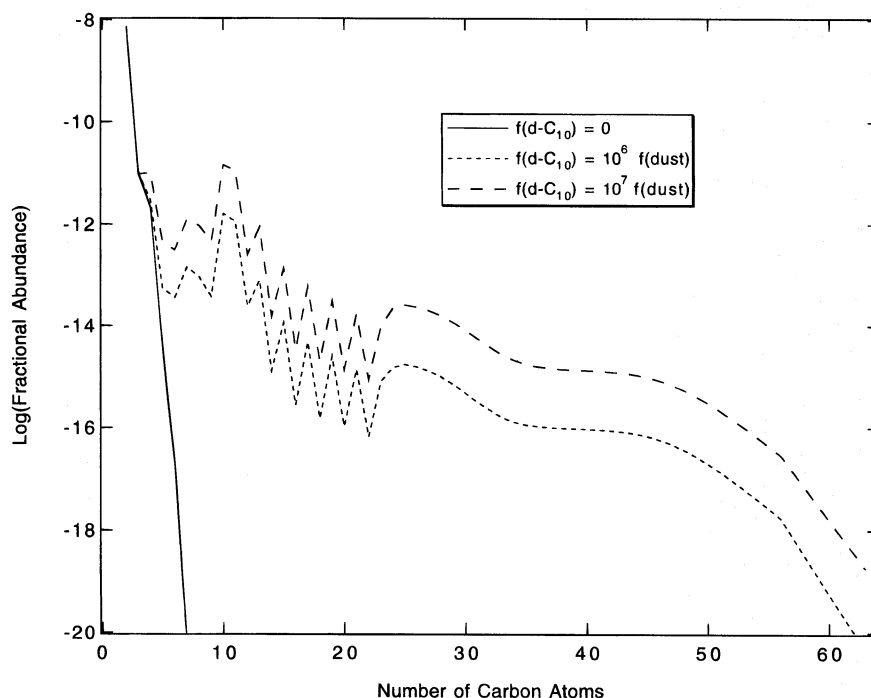


FIG. 6.—Graph of the log of fractional abundance of  $\text{C}_n\text{H}$  vs.  $n$  for the linear and monocyclic  $\text{C}_n\text{H}$  species at  $10^7 \text{ yr}$  using extended reaction set NSM with adsorbed seed molecules and  $A = 10^{-15} \text{ s}^{-1}$  under expanded cloud conditions.

ation and conversion reactions subsequently produce tricyclic rings and fullerenes, respectively. The model terminates at species with 64 carbon atoms. We have extended two reaction networks—the NSM (new standard model) network, which contains only a small number of neutral-neutral reactions, and the M4 (model 4) network, which contains a larger number of such reactions, although it excludes destructive reactions between oxygen atoms and bare carbon clusters. The M4 network produces larger abundances of complex molecules than does the NSM network.

The production of very complex molecules in interstellar clouds requires the existence of seed molecules, which can be polyatomic molecules with sizes through  $\approx 10$  atoms. Such molecules cannot be produced in the diffuse interstellar medium, because they are not stable against the strong interstellar radiation field. In most of our models, we have ignored the dust particles and utilized dynamical parameters corresponding to dispersive clouds, which begin life as dense clouds and disperse with various expansion velocities. Our results show that seed molecules produced under relatively dark cloud conditions lead to the production of far larger species, but that these species do not survive the diffuse interstellar medium with two exceptions: (1) molecules with 64 (or more) carbon atoms and (2) 60 carbon atom fullerenes ( $\text{f-C}_{60}$  and  $\text{f-C}_{60}^+$ ) and fulleranes ( $\text{f-C}_{60}\text{H}_m$  and  $\text{f-C}_{60}\text{H}_m^+$ ;  $m \geq 1$ ). Although large abundances

for the group of 64 carbon atom molecules can be produced with both extended reaction networks, only the M4 network leads to large predicted abundances for the fullerenes/anes. The 60 carbon atom fullerenes and very large molecules are reasonable candidates for carriers of the DIBs, although the group of very large species may encompass too many species for any one to be a viable candidate. The tentative assignment of two DIBs to the singly ionized fullerene  $\text{f-C}_{60}^+$  by Foing & Ehrenfreund (1994) is consistent with our results only if there is also a large abundance of the neutral fullerene, which may exceed the upper limit obtained from negative observations.

If, instead of a purely gas-phase model, we introduce seeds of adsorbed molecules on grain surfaces, which were presumably formed under static dense cloud conditions, and allow these species to photodesorb at a slow rate once the visual extinction decreases, we are able to produce large and sustainable abundances of both linear and monocyclic hydrocarbons, especially species with chemical formula  $\text{C}_n\text{H}_2$ ,  $n \leq 64$ . These and other unsaturated hydrocarbons must also be regarded as reasonable candidates to be carriers of the DIBs.

We acknowledge the support of the National Science Foundation for our research program in interstellar chemistry. We also thank the Ohio Supercomputer Center for computer time on their Cray Y-MP/8.

#### REFERENCES

- Bettens, R. P. A., & Herbst, E. 1995, *Int. J. Mass Spectrom. Ion Processes*, 149/150, 321  
 Bettens, R. P. A., Lee, H.-H., & Herbst, E. 1995, *ApJ*, 443, 664  
 Christian, J. F., Wan, Z., & Anderson, S. L. 1992, *J. Phys. Chem.*, 96, 3574  
 Crawford, M. K., Tielens, A. G. G. M., & Allamandola, L. J. 1985, *ApJ*, 293, L45  
 Douglas, A., E. 1977, *Nature*, 269, 130  
 Foing, B. H., & Ehrenfreund, P. 1994, *Nature*, 369, 296  
 Fulara, J., Lessen, D., Freivogel, P., & Maier, J. P. 1993, *Nature*, 366, 439  
 Hall, P., & Williams, D. A. 1995, *Ap&SS*, 229, 49  
 Herbig, G. H. 1993, *ApJ*, 407, 142  
 Herbst, E. 1991, *ApJ*, 366, 133  
 ———. 1996, in *Atomic, Molecular, and Optical Physics Reference Book*, ed. G. Drake (New York: AIP), 429  
 Herbst, E., & Leung, C. M. 1986, *ApJ*, 310, 378  
 ———. 1989, *ApJS*, 69, 271  
 ———. 1990, *A&A*, 233, 177  
 Hunter, J. M., Fye, J. L., Roskamp, E. J., & Jarrold, M. F. 1994, *J. Phys. Chem.*, 98, 1810  
 Léger, A., & d'Hendecourt, L. B. 1985, *A&A*, 146, 81  
 Maier, J. P. 1994, *Nature*, 370, 423  
 Petrie, S., Javahery, G., Wang, J., & Bohme, D. K. 1992, *J. Am. Chem. Soc.*, 114, 6268  
 Roueff, E. 1996, private communication  
 Sims, I. R., & Smith, I. W. M. 1995, *Annu. Rev. Phys. Chem.*, 46, 109  
 Snow, T. P., & Seab, C. G. 1989, *A&A*, 213, 291  
 Somerville, W. B., & Bellis, J. G. 1989, *MNRAS*, 240, 41P  
 Thaddeus, P. 1994, in *AIP Conf. Proc. 312, Molecules and Grains in Space*, ed. I. Nenner & L. Trojanowski (New York: AIP), 711  
 Van der Zwet, G. P., & Allamandola, L. J. 1985, *A&A*, 146, 76  
 von Helden, G., Gotts, N. G., & Bowers, M. T. 1993, *Nature*, 363, 60  
 Webster, A. 1992a, *A&A*, 257, 750  
 ———. 1992b, *MNRAS*, 255, 37P  
 ———. 1992c, *MNRAS*, 255, 41P  
 ———. 1993, *MNRAS*, 265, 421.  
 Woon, D. E., & Herbst, E. 1996, *ApJ*, 465, 795